Available online at www.sciencedirect.com
ScienceDirect
Journal of Power Sources 160 (2006) 1131–1141
JOURNAL OF POWER SOURCES
www.elsevier.com/locate/jpowsour

A mathematical model for simulating methanol permeation and the mixed potential effect in a direct methanol fuel cell

Chih-Hao Chen *, Tsung-Kuang Yeh

Nuclear Science and Technology Development Center, National Tsing Hua University, Taiwan

Received 10 February 2006; received in revised form 2 March 2006; accepted 3 March 2006
Available online 27 April 2006

Abstract

A mathematical model for simulating methanol permeation and the pertinent mixed potential effect in a direct methanol fuel cell (DMFC) is presented. In this model a DMFC is divided into seven compartments namely the anodic flow channel, the anodic diffusion layer, the anodic catalyst layer, the proton exchange membrane (PEM), the cathodic catalyst layer, the cathodic diffusion layer and the cathodic flow channel. All compartments are considered to have finite thickness, and within every one of them a set of governing equations are given to stipulate methanol transport and oxygen transport. For the flow channels, fluid dynamics, which could substantially lower the local methanol concentration within catalyst layers is taken into account. With the knowledge of local concentrations of the species, the electrochemical reaction rates within both catalyst layers can be quantified by a kinetic Tafel expression. For the anodic catalyst layer the local external current generated by methanol oxidation is computed; for the cathodic catalyst layer, in addition to the local external current generated by oxygen reduction, the local internal current as a result of methanol permeation is also computed. With the information of the local internal current, the mixed potential effect, which is responsible for adversely lowering the cell voltage can be analyzed.

Keywords: Direct methanol fuel cell; DMFC; Simulation; Modeling; Methanol permeation; Mixed potential

1. Introduction

The advantages of direct methanol fuel cells (DMFC) over hydrogen fuel cells include easy storage of the high energy density liquid fuel, direct fuel feeding without reforming, and low operating temperature. It is therefore considered by many people the most promising alternative power source for mobile applications and electric vehicles.

As shown schematically in Fig. 1, the structure a DMFC consists of seven major compartments namely the anodic flow channel, the anodic diffusion layer, the anodic catalyst layer, the proton exchange membrane (PEM), the cathodic catalyst layer, the cathodic diffusion layer and the cathodic flow channel. The anodic flow channel is the passage of low concentration methanol solution. As the solution is pumped through the channel, a small fraction of methanol diffuses through the anodic diffusion layer and reaches the anodic catalyst layer. Within this layer, where Pt–Ru is the most widely used catalyst today, methanol oxidizes and produces carbon dioxide (CO_2) via the following reaction:

$$CH_3OH + H_2O \rightarrow CO_2 + 6H^+ + 6e^-.$$

CO_2 then diffuses back into the anodic flow channel and exits with the solution. The protons, which travel through the PEM, and the electrons, which travel through some external load, reach the cathodic catalyst layer, where Pt is the catalyst, to undergo the following half-cell reaction with oxygen that comes from the cathodic flow channel:

$$3/2O_2 + 6H^+ + 6e^- \rightarrow 3H_2O.$$

Because these electrons travel through the external load, the pertinent current is referred to as the 'external' current in this paper. The overall reaction can therefore be written as:

$$CH_3OH + 3/2O_2 \rightarrow CO_2 + 2H_2O.$$

Despite its advantages over hydrogen fuel cells, a few engineering obstacles of the DMFC remain to be overcome. On the one hand, the sluggish catalytic activity of the anode makes a

* Corresponding author. Tel.: +886 3 5742865; fax: +886 3 5713849.
E-mail address: chih_hao_chen@yahoo.com (C.-H. Chen).

0378-7753/$ – see front matter © 2006 Elsevier B.V. All rights reserved.
doi:10.1016/j.jpowsour.2006.03.005

Nomenclature

A_{cell} cell area
$C^{feed}_{CH_3OH}$ methanol feed concentration
$C^{ref}_{CH_3OH}$ reference methanol concentration
C_{CH_3OH} local methanol concentration
$C^{vap}_{CH_3OH}$ gaseous methanol concentration at saturated vapor pressure
C_{H_2O} local water concentration
$C^{feed}_{O_2}$ oxygen feed concentration
$C^{ref}_{O_2}$ reference oxygen concentration
C_{O_2} local oxygen concentration
d_{af} width of the anodic flow channel
d_{cf} width of the anodic flow channel
D_{CH_3OH,H_2O} bulk diffusion coefficient of methanol in water
$D_{CH_3OH,air}$ bulk diffusion coefficient of gaseous methanol in air
$D_{CH_3OH,PEM}$ diffusion coefficient of methanol in PEM
$D_{O_2,air}$ bulk diffusion coefficient of oxygen in air
$D^{d,eff}_{CH_3OH,H_2O}$ effective diffusion coefficient of methanol in diffusion layers
$D^{ac,eff}_{CH_3OH,H_2O}$ effective diffusion coefficient of methanol in the anodic catalyst layer
$D^{cc,eff}_{CH_3OH,H_2O}$ effective diffusion coefficient of methanol in the cathodic catalyst layer
$D^{d,eff}_{O_2,air}$ effective diffusion coefficient of oxygen in diffusion layers
$D^{cc,eff}_{O_2,air}$ effective diffusion coefficient of oxygen in the cathodic catalyst layer
E difference of electrode potentials in a DMFC
f_{af} flow rate of anodic flow channel
f_{cf} flow rate of cathodic flow channel
j^{e}_{cell} cell external current density
j^{i}_{cell} cell internal current density
F Faraday's constant
j_{O_2} local current density from oxygen reduction
$j^{e}_{CH_3OH}$ local external current density from methanol oxidization
$j^{a,ref}_{0,CH_3OH}$ reference exchange current density of methanol in the anode
$j^{c,ref}_{0,CH_3OH}$ reference exchange current density of methanol in the cathode
$j^{e}_{O_2}$ local external current density from oxygen reduction
$j^{c,ref}_{0,O_2}$ reference exchange current density of oxygen in the cathode
$l^{a,ref}_{CH_3OH}$ reference catalyst layer thickness for methanol in the anode
$l^{c,ref}_{CH_3OH}$ reference catalyst layer thickness for methanol in the cathode
$l^{c,ref}_{O_2}$ reference catalyst layer thickness for oxygen in the cathode
l_{af} thickness of the anodic flow channel
l_{ad} thickness of the anodic diffusion layer
l_{ac} thickness of the anodic catalyst layer
l_{m} thickness of the PEM
l_{cc} thickness of the cathodic catalyst layer
l_{cd} thickness of the cathodic diffusion layer
l_{cf} thickness of the cathodic flow channel
M_{CH_3OH} molecular weight of methanol
M_{H_2O} molecular weight of water
n_{CH_3OH} number of transferred electrons per methanol molecule
n_{O_2} number of transferred electrons per water molecule
N_{CH_3OH} local methanol flux
N_{O_2} local oxygen flux
N_{H_2O} local water flux
r^{i}_{cell} cell interfacial resistence
V_{cell} cell output voltage
$w_{CH_3OH,a}$ decay width of methanol concentration along the anodic flow channel
$w_{CH_3OH,c}$ decay width of methanol concentration along the cathodic flow channel
$w_{O_2,c}$ decay width of oxygen concentration along the cathodic flow channel

Greek letters

α^{a}_{a,CH_3OH} anodic transfer coefficient of methanol in the anode
α^{c}_{a,CH_3OH} anodic transfer coefficient of methanol in the cathode
α^{a}_{c,CH_3OH} cathodic transfer coefficient of methanol in the anode
α^{c}_{c,CH_3OH} cathodic transfer coefficient of methanol in the cathode
α^{c}_{a,O_2} anodic transfer coefficient of oxygen in the cathode
α^{c}_{c,O_2} cathodic transfer coefficient of oxygen in the cathode
ε^{d} void fraction of diffusion layers
ε^{ac}_{s} volume fraction of solid phase in anodic catalyst layer
ε^{cc}_{s} volume fraction of solid phase in cathodic catalyst layer
ε^{c}_{m} volume fraction of ionomer phase in catalyst layers
γ_{O_2} reaction order of oxygen
$\gamma^{a}_{CH_3OH}$ reaction order of methanol in the anode
$\gamma^{c}_{CH_3OH}$ reaction order of methanol in the cathode
$\gamma^{c}_{O_2}$ reaction order of oxygen in the cathode
$\eta^{e}_{CH_3OH}$ local external overpotential of methanol
η_{O_2} local overpotential of oxygen
$\eta^{e}_{O_2}$ local external overpotential of oxygen
κ_{m} specific conductivity of the PEM
$\kappa^{ac,eff}_{s}$ effective conductivity of solid phase in the anodic catalyst layer

$\kappa_s^{cc,eff}$	effective conductivity of solid phase in the cathodic catalyst layer
$\kappa_m^{c,eff}$	effective conductivity of ionomer phase in catalyst layers
κ_s^{ac}	conductivity of solid phase in the anodic catalyst layer
κ_s^{cc}	conductivity of solid phase in the cathodic catalyst layer
κ_m^{c}	conductivity of ionomer phase in catalyst layers
λ_{H_2O}	drag coefficient of water
ρ_{CH_3OH}	density of methanol
ρ_{H_2O}	density of water

higher methanol concentration favorable. On the other hand the methanol permeation problem, which does not exist in hydrogen fuel cells, generates a mixed potential at the cathode and adversely lowers the cell output voltage at higher methanol concentration. Carbon monoxide (CO) poisoning poses another problem by reducing the electrocatalytic activity and active area of the catalyst. Another important issue is that methanol transport may be hindered by CO_2 that diffuses back into the anodic flow channel after being released within the anodic catalyst layer.

Methanol permeation is considered the most serious problem. The PEM is fully or almost fully hydrated when a DMFC is operating and methanol can therefore diffuse through the PEM and reach the cathodic catalyst layer. The catalyst in the cathode, which is made of Pt and adopted to reduce oxygen, also oxidizes the permeating methanol at the same time. Since the exchanged electrons in these redox reactions do not go through any external load, we refer to this current as the 'internal' current. How this internal current influences the performance of a DMFC is explained in the following. The cell output voltage V is related to the potential difference E by:

$$V = E - \eta_a - \eta_c - IR,$$

where η_a and η_c are the activation overpotentials of the anode and the cathode, respectively, and IR is the ohmic loss. The cathodic catalyst layer is assumed to be of zero thickness. Since the total amount of reduced oxygen must account for both the internal current density i^i and the external current density i^e, η_c is stipulated by the following Buttler-Volmer equation:

$$i^i + i^e = i_0 \left[\exp\left(\frac{\eta_c}{b_a}\right) - \exp\left(\frac{\eta_c}{b_c}\right) \right],$$

where b_a and b_c are the Tafel slopes of oxygen oxidation and reduction, respectively. If we keep i^e constant and raise i^i, η_c will be raised and therefore V will be lowered. Because contributions from i^i and i^e to η_c are mixed together and cannot be separated, η_c is usually referred to as the mixed potential.

Performance of a DMFC relies on a vast number of parameters, including the methanol feed concentration, efficiencies of methanol transport and oxygen transport within the compartments, the release rate of gaseous CO_2 and its effect on methanol transport, the specific area of catalyst in the catalyst layers, the thickness of the compartments, the impedance of the catalyst layer, the impedance of the membrane, the design of flow channels, the rate of methanol permeation and so on. Investigating the impact of these parameters one by one through experiments is not time or cost efficient. In order to help understand the operation of a DMFC and locate the key parameters on cell performance, a theoretical model is essential. A number of such models already exist in the literature.

Scott et al. [1] presented a DMFC model which accounts for the influence of methanol transport and of CO_2 flow. The model considers hydrodynamics in the flow channels associated with the production of CO_2 (in an empirical way) and methanol transport within the anodic diffusion layer, the anodic catalyst layer and the PEM. Within the PEM water transport is accounted for

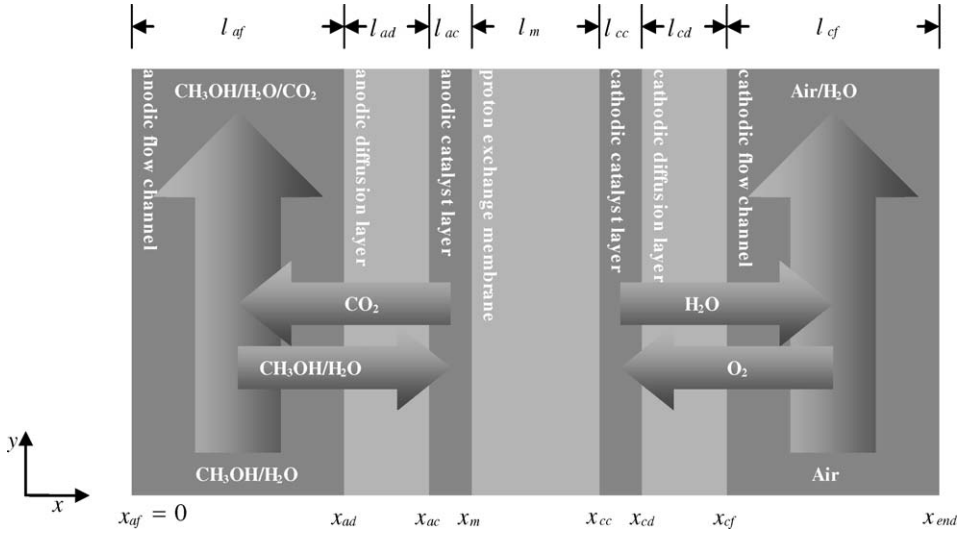

Fig. 1. Schematic of the DMFC which is divided into seven compartments namely the anodic flow channel, the anodic diffusion layer, the anodic catalyst layer, the PEM, the cathodic catalyst layer, the cathodic diffusion layer and the cathodic flow channel.

by diffusion and electro-osmotic drag. Within the anodic catalyst layer, methanol oxidation is accounted for by Tafel type kinetics. Experimental data were used for validation. Mass transport in the anode is found to be a factor that may limit the performance of the fuel cell. The open circuit potential as a result of methanol permeation is incorporated with a semi-empirical equation instead of theoretical analysis.

Jeng and Chen [2] reported a model for the anode of a DMFC. In the anodic flow channel, methanol transport associated with the production of CO_2 is accounted for in an empirical way. Diffusion and convection account for methanol transport and water transport in the diffusion layer as well as in the catalyst layer. Within the PEM water transport is accounted for by diffusion and electro-osmotic drag while methanol transport is accounted for in a similar way as in the diffusion layer. The electrochemical reaction in the catalyst layer is stipulated by a kinetic Tafel expression. The mixed potential effect is not addressed.

Meyers and Newman [3] developed a thermodynamic framework with which they are able to model the multi-component transport of species within the PEM [4]. In this model the authors quantify the gradients of electrochemical potential to describe the driving forces for the multi-component transport. In addition, a kinetic model considering multiple reaction steps is developed to describe methanol oxidation on the catalysts. With this model, a simulation of the direct methanol fuel cell is carried out and general aspects of its design are quantified [5]. The mixed potential effect is again not addressed.

In Divisek et al. [6], the authors developed and tested a two-dimensional model of a DMFC. In their model, the water transport is assumed to follow a standard two-phase flow mechanism, which can be seen as a generalized Darcy's law. The interactions between the gases and the ones between the gases and the pore walls are also taken into consideration. The mass transport of dissolved species is accounted for with a standard transport model. For charged species, appropriate potential equations are used. Energy considerations are derived from the Fourier law, with convection caused by the flow of fluids and gases. Electrochemical reactions are accounted for with methanol and oxygen kinetics. Condensation and evaporation processes are also considered. Although methanol permeation is considered, the mixed potential effect is not addressed.

In Wang and Wang [17], two-phase mass transfer is considered in the cathode (water and oxygen) and in the anode (methanol solution and CO_2) of a DMFC. Oxygen reduction and methanol oxidation are accounted for by Tafel kinetic equations. Simulation results show that cell performance relies heavily on methanol feed concentrations. With small methanol feed concentrations the cell suffers from low limiting current densities. For feed concentrations below 1 M, an increase in methanol concentration leads to a small decrease in cell voltage. For a feed concentration larger than 2 M, the cell voltage is reduced substantially by excessive methanol permeation and the maximum current is limited by the oxygen depletion at the cathode. The mixed potential effect as a result of methanol permeation is taken into account by assuming that the methanol transported to the cathode is completely depleted.

The mixed potential effect is not easy to simulate and, in the models mentioned above, is unaddressed, calculated in an empirical way or handled with a simple assumption of full depletion of the permeating methanol by the cathode. Empirical approaches are often useful in correlating experimental data if the model contains sufficient insights of the system, but are less helpful on the investigation of cell parameters or on the effects of changing cell designs. The assumption of full depletion of the permeating methanol by the cathode may not always be true, especially when the catalytic activity of the cathode is not so efficient, as found out and discussed in the Results and Discussion section. The mathematical model, which is proposed here is based upon the description of the physicochemical processes which dictate the behavior of electrochemical systems, namely, mass transport and reaction kinetics. The features that distinguish our model from the foregoing ones are:

1. fluid dynamics of the flow channels which may influence the concentrations of species at the catalyst layers, change the reaction rates and impact the performance of the cell,
2. mass transport and reaction kinetics of the cathode, and
3. a means to estimating the intensity of the internal current, the mixed potential effect and consequently the impact on cell output voltage.

2. Theory and calculation

Our model is based on the following set of assumptions:

1. The fuel cell is operated isothermally at 30 °C in a steady state.
2. There is no pressure difference between the compartments.
3. Methanol flux into the anodic flow channel is much greater than methanol flux into the anodic diffusion layer. This ensures that methanol concentration variation is small along the channel. The same assumption applies to oxygen flux in the cathodic flow channel.
4. The effects of generated products, carbon dioxide and water, on methanol transport and on oxygen transport are neglected.

Furthermore, as will be discussed in the next section, the reduction in the electrocatalytic activity and active reaction area of the catalyst due to CO poisoning is accounted for by selecting appropriate reference exchange current densities, namely $j^{a,ref}_{0,CH_3OH}$, $j^{c,ref}_{0,CH_3OH}$ and $j^{c,ref}_{0,O_2}$. However, it should be noted that, since we only discuss steady-state operations, the transient effect of CO poisoning on these exchange current densities is not included in this model.

A variable map is presented in Table 1. The concentration and flux of methanol, C_{CH_3OH} and N_{CH_3OH}, are considered all over the cell. The concentration and flux of oxygen, C_{O_2} and N_{O_2}, are considered only in the cathode because oxygen does not penetrate the PEM. Within the anodic catalyst layer where methanol oxidizes, the external current density from methanol oxidation $j^{e}_{CH_3OH}$ and its activation overpotential $\eta^{e}_{CH_3OH}$ are added. Within the cathodic catalyst layer, in addition to the external

Table 1
Variable map showing the variables which are solved for in the seven compartments of the DMFC

	Anodic flow channel	Anodic diffusion layer	Anodic catalyst layer	PEM	Cathodic catalyst layer	Cathodic diffusion layer	Cathodic flow channel
C_{CH_3OH}	√	√	√	√	√	√	√
N_{CH_3OH}	√	√	√	√	√	√	√
C_{O_2}					√	√	√
N_{O_2}					√	√	√
N_{H_2O}	√	√	√	√	√	√	
$j^e_{CH_3OH}$			√				
$\eta^e_{CH_3OH}$			√				
$j^e_{O_2}$					√		
$\eta^e_{O_2}$					√		
j_{O_2}					√		

current density from oxygen reduction $j^e_{O_2}$ and its activation overpotential $\eta^e_{O_2}$, the total current density from oxygen reduction j_{O_2} is needed to account for the internal currents. Our choice differs from other approaches in the literature and substantially simplifies the governing equations and the boundary conditions.

2.1. Governing equations

The following notations are used to simplify the governing equations. $B_s(C, \eta)$ is the abbreviation of the kinetic Tafel expression:

$$B^l_s(C,\eta) = \frac{j^{l,ref}_{0,s}}{l^{l,ref}_s}\left(\frac{C}{C^{l,ref}_s}\right)^{\gamma^l_s} \times \left(\exp\left(\frac{\alpha^l_{a,s} n_s F}{RT}\eta\right) - \exp\left(-\frac{\alpha^l_{c,s} n_s F}{RT}\eta\right)\right),$$

where s stands for species (CH_3OH or O_2) and l for location (a for anode or c for cathode). Effective diffusion coefficients (Ds) and effective conductivities (κs) are defined as:

$$D^{d,eff}_{CH_3OH,H_2O} = (\varepsilon^d)^{3/2} D_{CH_3OH,H_2O},$$

$$D^{ac,eff}_{CH_3OH,H_2O} = (1-\varepsilon^{ac}_s-\varepsilon^c_m)^{3/2} D_{CH_3OH,H_2O},$$

$$D^{cc,eff}_{CH_3OH,H_2O} = (1-\varepsilon^{cc}_s-\varepsilon^c_m)^{3/2} D_{CH_3OH,H_2O}$$

$$D^{cc,eff}_{O_2,Air} = (1-\varepsilon^{cc}_s-\varepsilon^c_m)^{3/2} D_{O_2,Air},$$

$$\kappa^{ac,eff}_s = (\varepsilon^{ac}_s)^{3/2}\kappa^{ac}_s, \qquad \kappa^{cc,eff}_s = (\varepsilon^{cc}_s)^{3/2}\kappa^{cc}_s,$$

$$\kappa^{eff}_m = (\varepsilon^c_m)^{3/2}\kappa_m,$$

using Bruggeman's correction [7–9]. The derivation of the governing equations in the seven compartments of a DMFC is shown below.

2.1.1. The anodic flow channel

In this compartment methanol flux results from diffusion and convection:

$$N_{CH_3OH} = N^{diff}_{CH_3OH} + N^{conv}_{CH_3OH},$$

where

$$N^{conv}_{CH_3OH} = \frac{M_{H_2O} C_{CH_3OH}|_{x=x_{ad}} N_{H_2O}|_{x=x_{ad}}}{\rho_{H_2O}},$$

and

$$N^{diff}_{CH_3OH} = -D_{CH_3OH,H_2O}\frac{dC_{CH_3OH}}{dx}.$$

The last equation can be reorganized as:

$$\frac{dC_{CH_3OH}}{dx} = -\frac{N^{diff}_{CH_3OH}}{D_{CH_3OH,H_2O}}. \quad (1)$$

This reorganization is also applied to mass transfer in all the other compartments.

By fluid dynamics and mass transfer calculation in Appendix A, $N^{diff}_{CH_3OH}$ must satisfy the following equation:

$$\frac{dN^{diff}_{CH_3OH}}{dx} = \frac{6 f_{af}}{w_{CH_3OH,a} d_{af} l^3_{af}}(x - x_{af})(l_{af} - x + x_{af}) C_{CH_3OH}. \quad (2)$$

2.1.2. The anodic diffusion layer

In this compartment, methanol transfer is driven by diffusion and convection:

$$\frac{dC_{CH_3OH}}{dx} = -\frac{N_{CH_3OH}}{D^{d,eff}_{CH_3OH,H_2O}} + \frac{M_{H_2O} N_{H_2O} C_{CH_3OH}}{D^{d,eff}_{CH_3OH,H_2O}\rho_{H_2O}}. \quad (3)$$

Because no electrochemical reactions occur, the methanol flux and the water flux are constant:

$$\frac{dN_{CH_3OH}}{dx} = 0, \quad (4)$$

$$\frac{dN_{H_2O}}{dx} = 0. \quad (5)$$

2.1.3. The anodic catalyst layer

In this compartment, methanol transfer is a result of diffusion and convection:

$$\frac{dC_{CH_3OH}}{dx} = -\frac{N_{CH_3OH}}{D^{ac,eff}_{CH_3OH,H_2O}} + \frac{M_{H_2O} N_{H_2O} C_{CH_3OH}}{D^{ac,eff}_{CH_3OH,H_2O}\rho_{H_2O}}. \quad (6)$$

Methanol oxidation which, can be stipulated by a kinetic Tafel expression changes the methanol flux and the water flux:

$$\frac{\mathrm{d}j^{\mathrm{e}}_{\mathrm{CH_3OH}}}{\mathrm{d}x} = B^{\mathrm{a}}_{\mathrm{CH_3OH}}(C_{\mathrm{CH_3OH}}, \eta^{\mathrm{e}}_{\mathrm{CH_3OH}}), \tag{7}$$

$$\frac{\mathrm{d}N_{\mathrm{CH_3OH}}}{\mathrm{d}x} = -\frac{1}{n_{\mathrm{CH_3OH}}F}\frac{\mathrm{d}j^{\mathrm{e}}_{\mathrm{CH_3OH}}}{\mathrm{d}x}, \tag{8}$$

$$\frac{\mathrm{d}N_{\mathrm{H_2O}}}{\mathrm{d}x} = \frac{\mathrm{d}N_{\mathrm{CH_3OH}}}{\mathrm{d}x}, \tag{9}$$

$\eta^{\mathrm{e}}_{\mathrm{CH_3OH}}$, the external overpotential by methanol, is changed by the electron flow in solid phase and the proton flow in ionomer phase [2]:

$$\frac{\mathrm{d}\eta^{\mathrm{e}}_{\mathrm{CH_3OH}}}{\mathrm{d}x} = \left(\frac{1}{\kappa^{\mathrm{c,eff}}_{\mathrm{m}}} + \frac{1}{\kappa^{\mathrm{ac,eff}}_{\mathrm{s}}}\right) j^{\mathrm{e}}_{\mathrm{CH_3OH}} - \frac{1}{\kappa^{\mathrm{ac,eff}}_{\mathrm{s}}} j^{\mathrm{e}}_{\mathrm{cell}}. \tag{10}$$

2.1.4. The PEM

In this compartment, methanol transfer is caused by diffusion and convection:

$$\frac{\mathrm{d}C_{\mathrm{CH_3OH}}}{\mathrm{d}x} = -\frac{N_{\mathrm{CH_3OH}}}{D_{\mathrm{CH_3OH,PEM}}} + \frac{M_{\mathrm{H_2O}}N_{\mathrm{H_2O}}C_{\mathrm{CH_3OH}}}{D_{\mathrm{CH_3OH,PEM}}\rho_{\mathrm{H_2O}}}. \tag{11}$$

No electrochemical reaction occurs in this compartment to change the methanol flux or the water flux:

$$\frac{\mathrm{d}N_{\mathrm{CH_3OH}}}{\mathrm{d}x} = 0, \tag{12}$$

$$\frac{\mathrm{d}N_{\mathrm{H_2O}}}{\mathrm{d}x} = 0, \tag{13}$$

We further assume that the PEM is fully hydrated so that water concentration is constant and that no water diffusion takes place.

2.1.5. The cathodic catalyst layer

In this compartment, methanol transfer is due to diffusion and convection:

$$\frac{\mathrm{d}C_{\mathrm{CH_3OH}}}{\mathrm{d}x} = -\frac{N_{\mathrm{CH_3OH}}}{D^{\mathrm{cc,eff}}_{\mathrm{CH_3OH,H_2O}}} + \frac{M_{\mathrm{H_2O}}N_{\mathrm{H_2O}}C_{\mathrm{CH_3OH}}}{D^{\mathrm{cc,eff}}_{\mathrm{CH_3OH,H_2O}}\rho_{\mathrm{H_2O}}}. \tag{14}$$

Oxygen transfer is a result of diffusion:

$$\frac{\mathrm{d}C_{\mathrm{O_2}}}{\mathrm{d}x} = -\frac{N_{\mathrm{O_2}}}{D^{\mathrm{cc,eff}}_{\mathrm{O_2,air}}}. \tag{15}$$

Oxygen reduction generates both the external current and the internal current. The combination of both and the former along are stipulated by kinetic Tafel expressions:

$$\frac{\mathrm{d}j_{\mathrm{O_2}}}{\mathrm{d}x} = B^{\mathrm{c}}_{\mathrm{O_2}}(C_{\mathrm{O_2}}, \eta_{\mathrm{O_2}}), \tag{16}$$

$$\frac{\mathrm{d}j^{\mathrm{e}}_{\mathrm{O_2}}}{\mathrm{d}x} = B^{\mathrm{c}}_{\mathrm{O_2}}(C_{\mathrm{O_2}}, \eta^{\mathrm{e}}_{\mathrm{O_2}}). \tag{17}$$

The methanol flux, the oxygen flux and the water flux all change accordingly with the generation of these current densities:

$$\frac{\mathrm{d}N_{\mathrm{O_2}}}{\mathrm{d}x} = \frac{1}{n_{\mathrm{O_2}}F}\frac{\mathrm{d}j_{\mathrm{O_2}}}{\mathrm{d}x}, \tag{18}$$

$$\frac{\mathrm{d}N_{\mathrm{CH_3OH}}}{\mathrm{d}x} = \frac{1}{n_{\mathrm{CH_3OH}}F}\left(\frac{\mathrm{d}j_{\mathrm{O_2}}}{\mathrm{d}x} - \frac{\mathrm{d}j^{\mathrm{e}}_{\mathrm{O_2}}}{\mathrm{d}x}\right), \tag{19}$$

$$\frac{\mathrm{d}N_{\mathrm{H_2O}}}{\mathrm{d}x} = \frac{\mathrm{d}N_{\mathrm{CH_3OH}}}{\mathrm{d}x} - 2\frac{\mathrm{d}N_{\mathrm{O_2}}}{\mathrm{d}x}. \tag{20}$$

Once again the electron flow in the solid phase and the proton flow in the ionomer phase change the external overpotential by oxygen $\eta^{\mathrm{e}}_{\mathrm{O_2}}$:

$$\frac{\mathrm{d}\eta^{e}_{\mathrm{O2}}}{\mathrm{d}x} = \left(\frac{1}{\kappa^{\mathrm{c,eff}}_{\mathrm{m}}} + \frac{1}{\kappa^{\mathrm{cc,eff}}_{\mathrm{s}}}\right) j^{\mathrm{e}}_{\mathrm{O_2}} - \frac{1}{\kappa^{\mathrm{cc,eff}}_{\mathrm{s}}} j^{\mathrm{e}}_{\mathrm{cell}}. \tag{21}$$

The sum of the methanol internal current density and the oxygen internal current density must be zero. Therefore, the following equation must hold all over this compartment:

$$\frac{\mathrm{d}j_{\mathrm{O_2}}}{\mathrm{d}x} - \frac{\mathrm{d}j^{\mathrm{e}}_{\mathrm{O_2}}}{\mathrm{d}x} + B^{\mathrm{c}}_{\mathrm{CH_3OH}}(C_{\mathrm{CH_3OH}}, E + \eta_{\mathrm{O_2}}) = 0. \tag{22}$$

2.1.6. The cathodic diffusion layer

In this compartment, methanol transfer is due to diffusion and convection:

$$\frac{\mathrm{d}C_{\mathrm{CH_3OH}}}{\mathrm{d}x} = -\frac{N_{\mathrm{CH_3OH}}}{D^{\mathrm{d,eff}}_{\mathrm{CH_3OH,H_2O}}} + \frac{M_{\mathrm{H_2O}}N_{\mathrm{H_2O}}C_{\mathrm{CH_3OH}}}{D^{\mathrm{d,eff}}_{\mathrm{CH_3OH,H_2O}}\rho_{\mathrm{H_2O}}}. \tag{23}$$

Oxygen transfer is a result of diffusion:

$$\frac{\mathrm{d}C_{\mathrm{O_2}}}{\mathrm{d}x} = -\frac{N_{\mathrm{O_2}}}{D^{\mathrm{d,eff}}_{\mathrm{O_2,air}}}. \tag{24}$$

No electrochemical reaction occurs to change the methanol flux, the oxygen flux or the water flux:

$$\frac{\mathrm{d}N_{\mathrm{CH_3OH}}}{\mathrm{d}x} = 0, \tag{25}$$

$$\frac{\mathrm{d}N_{\mathrm{O_2}}}{\mathrm{d}x} = 0, \tag{26}$$

$$\frac{\mathrm{d}N_{\mathrm{H_2O}}}{\mathrm{d}x} = 0. \tag{27}$$

2.1.7. The cathodic flow channel

In this compartment, methanol transfer and oxygen transfer can be derived as in the anodic flow channel:

$$\frac{\mathrm{d}N_{\mathrm{CH_3OH}}}{\mathrm{d}x} = -\frac{6f_{\mathrm{cf}}}{w_{\mathrm{CH_3OH,c}}d_{\mathrm{cf}}l^3_{\mathrm{cf}}}(x - x_{\mathrm{cf}})(x_{\mathrm{end}} - x)C_{\mathrm{CH_3OH}}, \tag{28}$$

$$\frac{\mathrm{d}C_{\mathrm{CH_3OH}}}{\mathrm{d}x} = -\frac{N_{\mathrm{CH_3OH}}}{D_{\mathrm{CH_3OH,air}}}, \tag{29}$$

$$\frac{\mathrm{d}N_{\mathrm{O_2}}}{\mathrm{d}x} = \frac{6f_{\mathrm{cf}}}{w_{\mathrm{O_2,c}}d_{\mathrm{cf}}l^3_{\mathrm{cf}}}(x - x_{\mathrm{cf}})(x_{\mathrm{end}} - x)C_{\mathrm{O_2}}, \tag{30}$$

$$\frac{\mathrm{d}C_{\mathrm{O_2}}}{\mathrm{d}x} = -\frac{N_{\mathrm{O_2}}}{D_{\mathrm{O_2,air}}}. \tag{31}$$

Note that methanol is in gas phase here.

2.2. Boundary conditions

A set of boundary conditions are required to solve the differential equations above.

2.2.1. At $x = x_{af}$

$$C_{CH_3OH} = C^{feed}_{CH_3OH}, \tag{32}$$

$$N^{diff}_{CH_3OH} = 0. \tag{33}$$

2.2.2. At $x = x_{ad}$

$$C_{CH_3OH} \quad \text{and} \quad N_{CH_3OH} \quad \text{arecontinuous.} \tag{34}$$

Water flux results from water consumption by the anodic catalyst layer and electro-osmosis in the PEM:

$$N_{H_2O} = \left(\frac{1}{n_{CH_3OH}} + \lambda_{H_2O}\right)\frac{j^e_{cell}}{F}. \tag{35}$$

2.2.3. At $x = x_{ac}$

$$C_{CH_3OH} \quad \text{and} \quad N_{CH_3OH} \quad \text{arecontinuous,} \tag{36}$$

$$j^e_{CH_3OH} = 0. \tag{37}$$

2.2.4. At $x = x_m$

$$C_{CH_3OH} \quad \text{and} \quad N_{CH_3OH} \quad \text{arecontinuous,} \tag{38}$$

$$j^e_{CH_3OH} = j^e_{cell}. \tag{39}$$

2.2.5. At $x = x_{cc}$

$$C_{CH_3OH} \quad \text{and} \quad N_{CH_3OH} \quad \text{arecontinuous,} \tag{40}$$

$$N_{O_2} = 0, \tag{41}$$

$$j_{O_2} = 0, \tag{42}$$

$$j^e_{O_2} = 0. \tag{43}$$

Eq. (41) comes from our assumption that oxygen does not penetrate the PEM and exists only in the cathode.

2.2.6. At $x = x_{cd}$

$$C_{CH_3OH}, N_{CH_3OH}, C_{O_2} \quad \text{and} \quad N_{O_2} \quad \text{arecontinuous,} \tag{44}$$

$$j^e_{O_2} = -j^e_{cell}. \tag{45}$$

2.2.7. At $x = x_{cf}$

$$N_{CH_3OH}, C_{O_2} \quad \text{and} \quad N_{O_2} \quad \text{arecontinuous.} \tag{46}$$

Methanol vaporizes at this boundary and its concentration in gas phase can be determined by its molar fraction in the solution:

$$\left[\frac{C_{CH_3OH}}{C^{vap}_{CH_3OH}}\right]_{x>x_{cf}} = \left[\frac{C_{CH_3OH}}{C_{CH_3OH} + C_{H_2O}}\right]_{x<x_{cf}}, \tag{47}$$

where can be determined by

$$\frac{M_{CH_3OH}C_{CH_3OH}}{\rho_{CH_3OH}} + \frac{M_{H_2O}C_{H_2O}}{\rho_{H_2O}} = 1.$$

2.2.8. At $x = x_{end}$

$$C_{O_2} = C^{feed}_{O_2}, \tag{48}$$

$$N_{O_2} = 0, \tag{49}$$

$$C_{CH_3OH} = 0, \tag{50}$$

$$N_{CH_3OH} = 0. \tag{51}$$

2.3. Numerical method

Eqs. (1)–(31) form a set of first-order differential equations, which can be readily solved with boundary conditions Eq. (32)–(51) by applying Runge-Kutta method of order 4. Because the boundary conditions are not at the same location, the solving procedure must include first guesses of variables and a large number of iterations to make the solution converge.

2.4. Determination of cell voltage

The total power density of the cell is

$$p_t = E(j^e_{cell} + j^i_{cell}).$$

The usable power density of the cell is

$$p_u = Vj^e_{cell}.$$

The power density of anodic activation is

$$p_{aa} = \int_{x_{ac}}^{x_m} \eta^e_{CH_3OH}\frac{dj^e_{CH_3OH}}{dx}dx.$$

The power density of cathodic activation is

$$p_{ac} = \int_{x_{ac}}^{x_m}(E + \eta_{O_2})\left(\frac{dj^e_{O_2}}{dx} - \frac{dj_{O_2}}{dx}\right)dx + \int_{x_{ac}}^{x_m}\eta_{O_2}\frac{dj_{O_2}}{dx}dx,$$

where the first term is for methanol and the second term for oxygen. The power density of *IR* loss is

$$\begin{aligned} p_{IR} = &\int_{x_{ac}}^{x_m}\left(\frac{(j^e_{CH_3OH})^2}{\kappa^{c,eff}_m} + \frac{(j^e_{cell} - j^e_{CH_3OH})^2}{\kappa^{ac,eff}_s}\right)dx \\ &+ \int_{x_{cc}}^{x_{cd}}\left(\frac{(j^e_{cell} + j^e_{O_2})^2}{\kappa^{c,eff}_m} + \frac{(j^e_{O_2})^2}{\kappa^{cc,eff}_s}\right)dx \\ &+ \frac{(j^e_{cell})^2}{\kappa_m}l_m + (j^e_{cell})^2 A_{cell}r^i_{cell}, \end{aligned}$$

where the first term is for the anodic catalyst layer, the second term for the cathodic catalyst layer[2], the third term for the PEM and the forth term for interfacial resistance. By conservation of power density,

$$p_u = p_t - p_{aa} - p_{ac} - p_{IR},$$

we then have

$$V_{\text{cell}} j^{\text{e}}_{\text{cell}} = E(j^{\text{e}}_{\text{cell}} + j^{\text{i}}_{\text{cell}}), \quad - \int_{x_{\text{ac}}}^{x_{\text{m}}} \eta^{\text{e}}_{\text{CH}_3\text{OH}} \frac{\text{d}\, j^{\text{e}}_{\text{CH}_3\text{OH}}}{\text{d}x}\, \text{d}x,$$
$$- \int_{x_{\text{ac}}}^{x_{\text{m}}} (E + \eta_{\text{O}_2}) \left(\frac{\text{d}\, j^{\text{e}}_{\text{O}_2}}{\text{d}x} - \frac{\text{d}\, j_{\text{O}_2}}{\text{d}x} \right) \text{d}x$$
$$- \int_{x_{\text{ac}}}^{x_{\text{m}}} \eta_{\text{O}_2} \frac{\text{d}\, j_{\text{O}_2}}{\text{d}x}\, \text{d}x,$$
$$- \int_{x_{\text{ac}}}^{x_{\text{m}}} \left(\frac{(j^{\text{e}}_{\text{CH}_3\text{OH}})^2}{\kappa^{\text{c,ef}f}_{\text{m}}} + \frac{(j^{\text{e}}_{\text{cell}} - j^{\text{e}}_{\text{CH}_3\text{OH}})^2}{\kappa^{\text{ac,eff}}_{\text{s}}} \right) \text{d}x$$
$$- \int_{x_{\text{cc}}}^{x_{\text{cd}}} \left(\frac{(j^{\text{e}}_{\text{cell}} + j^{\text{e}}_{\text{O}_2})^2}{\kappa^{\text{c,eff}}_{\text{m}}} + \frac{(j^{\text{e}}_{\text{O}_2})^2}{\kappa^{\text{cc,eff}}_{\text{s}}} \right) \text{d}x,$$
$$- \frac{(j^{\text{e}}_{\text{cell}})^2}{\kappa_{\text{m}}} l_{\text{m}} - (j^{\text{e}}_{\text{cell}})^2 A_{\text{cell}} r^{\text{i}}_{\text{cell}}.$$

After rearranging the terms and applying $\int_{x_{\text{ac}}}^{x_{\text{m}}} E \left(\frac{\text{d}\, j^{\text{e}}_{\text{O}_2}}{\text{d}x} - \frac{\text{d}\, j_{\text{O}_2}}{\text{d}x} \right) \text{d}x = E j^{\text{i}}_{\text{cell}}$ we have

$$V_{\text{cell}} j^{\text{e}}_{\text{cell}} = E j^{\text{e}}_{\text{cell}}, \quad - \int_{x_{\text{ac}}}^{x_{\text{m}}} \eta^{\text{e}}_{\text{CH}_3\text{OH}} \frac{\text{d}\, j^{\text{e}}_{\text{CH}_3\text{OH}}}{\text{d}x}\, \text{d}x,$$
$$- \int_{x_{\text{ac}}}^{x_{\text{m}}} \eta_{\text{O}_2} \frac{\text{d}\, j^{\text{e}}_{\text{O}_2}}{\text{d}x}\, \text{d}x,$$
$$- \int_{x_{\text{ac}}}^{x_{\text{m}}} \left(\frac{(j^{\text{e}}_{\text{CH}_3\text{OH}})^2}{\kappa^{\text{c,eff}}_{\text{m}}} + \frac{(j^{\text{e}}_{\text{cell}} - j^{\text{e}}_{\text{CH}_3\text{OH}})^2}{\kappa^{\text{ac,eff}}_{\text{s}}} \right) \text{d}x$$
$$- \int_{x_{\text{cc}}}^{x_{\text{cd}}} \left(\frac{(j^{\text{e}}_{\text{cell}} + j^{\text{e}}_{\text{O}_2})^2}{\kappa^{\text{c,eff}}_{\text{m}}} + \frac{(j^{\text{e}}_{\text{O}_2})^2}{\kappa^{\text{cc,eff}}_{\text{s}}} \right) \text{d}x,$$
$$- \frac{(j^{\text{e}}_{\text{cell}})^2}{\kappa_{\text{m}}} l_{\text{m}} - (j^{\text{e}}_{\text{cell}})^2 A_{\text{cell}} r^{\text{i}}_{\text{cell}}. \quad (52)$$

3. Results and discussion

In order to validate our model, a cell is assembled in our laboratory with which experimental data is generated and compared to model predictions. The catalyst layers of the cell are made of Nafion 117, Teflon-treated carbon clothes and commercial catalysts from Johnson Matthey with these weight ratios: Pt 20 wt.% and Ru 10 wt.% for the anode, Pt 20% for the cathode. Amounts of Pt usage on catalyst layers are 0.9 mg cm^{-2} for both the anode and the cathode. A membrane made of Nafion 117 is hot pressed between the catalyst layers at 130 °C to form the membrane electrode assembly (MEA). The MEA is then sandwiched between two graphite plates on which flow channels are carved. After the cell is assembled, we delineate its *I–V* characteristic curves at different methanol feed concentrations as shown in Fig. 2.

Next we determine key parameter values of the model through calibration, by fitting model-predicted *I–V* characteristic curves to experimental data. The best fitting, also shown in Fig. 2, is obtained with the set of parameter values listed in Table 2.

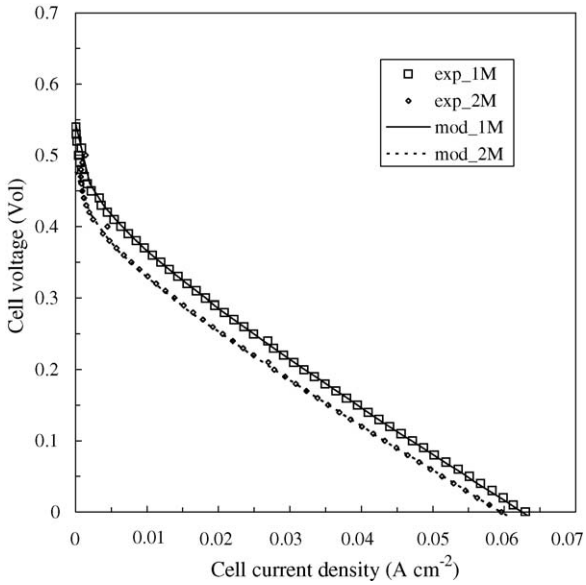

Fig. 2. Polarization curves of our cell compared with model predictions after calibration.

With key parameter values determined, the mixed potential effect can be analyzed by examining the difference between the cathodic activation overpotentials of oxygen with the internal current enabled and disabled. In the case of disabled internal current, the way methanol transport to the cathode is not changed while methanol oxidation within the cathodic catalyst layer is assumed not to take place. This difference, as shown in Fig. 3 where the methanol feed concentration is still 1 M, decreases as cell current density increases. This can be understood since higher cell current densities gives lower methanol flux into the cathode, as shown in Fig. 5, which will be discussed later. This

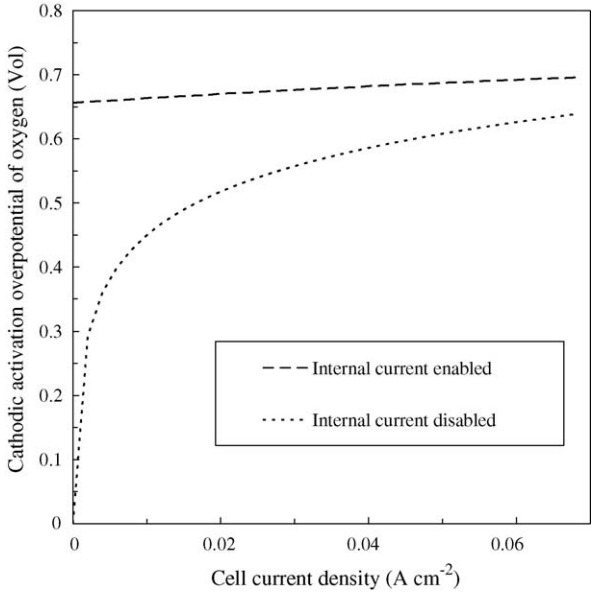

Fig. 3. Comparison of mixed potentials with internal current enabled and disabled at $C^{\text{feed}}_{\text{CH}_3\text{OH}} = 1$ M.

Table 2
Parameter values used in numerical simulations

Parameter	Value	Reference
A_{cell} (cm^2)	4	Measurement
D_{CH_3OH,H_2O} ($cm^2\,s^{-1}$)	1.93×10^{-5}	[10]
$D_{CH_3OH,air}$ ($cm^2 s^{-1}$)	1.569×10^{-1}	[11]
$D_{CH_3OH,PEM}$ ($cm^2\,s^{-1}$)	4.9×10^{-6}	[13]
$D_{O_2,air}$ ($cm^2\,s^{-1}$)	1.02×10^{1}	[10]
d_{af} (cm)	0.1	Measurement
d_{cf} (cm)	0.1	Measurement
f_{af} ($cm^3\,s^{-1}$)	0.83	Measurement
f_{cf} ($cm^3\,s^{-1}$)	1.66	Measurement
$j^{a,ref}_{0,CH_3OH}$ ($A\,cm^{-2}$)	4.5×10^{-4}	Calibration
$j^{c,ref}_{0,CH_3OH}$ ($A\,cm^{-2}$)	4.5×10^{-4}	Calibration
$l^{a,ref}_{CH_3OH}$ (cm)	0.03	Measurement
$l^{c,ref}_{CH_3OH}$ (cm)	0.03	Measurement
$j^{c,ref}_{0,O_2}$ ($A\,cm^{-2}$)	1×10^{-4}	Calibration
$l^{c,ref}_{O_2}$ (cm)	0.03	Measurement
l_{af} (cm)	0.1	Measurement
l_{ad} (cm)	0.03	Measurement
l_{ac} (cm)	0.001	Measurement
l_m (cm)	0.015	Measurement
l_{cc} (cm)	0.001	Measurement
l_{cd} (cm)	0.03	Measurement
l_{cf} (cm)	0.1	Measurement
r^i_{cell} (ohm)	1.4	Calibration
α^a_{a,CH_3OH}	0.153	Calibration
α^c_{a,CH_3OH}	0.153	Calibration
α^a_{c,CH_3OH}	0.12	Calibration
α^c_{c,CH_3OH}	0.12	Calibration
α^c_{a,O_2}	0.0669	Assumption
α^c_{c,O_2}	0.0669	[14]
$\gamma^a_{CH_3OH}$	1.4	Calibration
$\gamma^c_{CH_3OH}$	2	Calibration
$\gamma^c_{O_2}$	1	Calibration
κ^{ac}_s ($S\,cm^{-1}$)	8.13×10^{6}	[15]
κ^{cc}_s ($S\,cm^{-1}$)	8.13×10^{6}	Assumption
κ^c_m ($S\,cm^{-1}$)	1.416×10^{-1}	[13]
κ_m ($S\,cm^{-1}$)	8.3×10^{-2}	[16]
ε^d	7.06×10^{-1}	[2]
ε^{ac}_s	6×10^{-1}	[2]
ε^{cc}_s	6×10^{-1}	Assumption
ε^c_m	8×10^{-2}	[2]
λ_{H_2O}	2.36	[12]

also indicates that methanol permeation has a weaker impact on cell output voltage at higher cell current densities.

The model can further be used to predict methanol concentration distributions and methanol flux inside the cell at different cell current densities, as shown in Figs. 4 and 5 where the methanol feed concentration is fixed at 1 M. Because it is difficult to see these curves within the very thin cathodic catalyst layer, we show the magnified versions in the lower frames. Fig. 4 shows that the methanol concentrations fall substantially in the anodic flow channel just before the anodic diffusion layer. This result, which is just as expected, justifies the integration of flow channel calculation into our model. Regarding the cathodic flow channel, due to the high diffusion coefficient of oxygen in air,

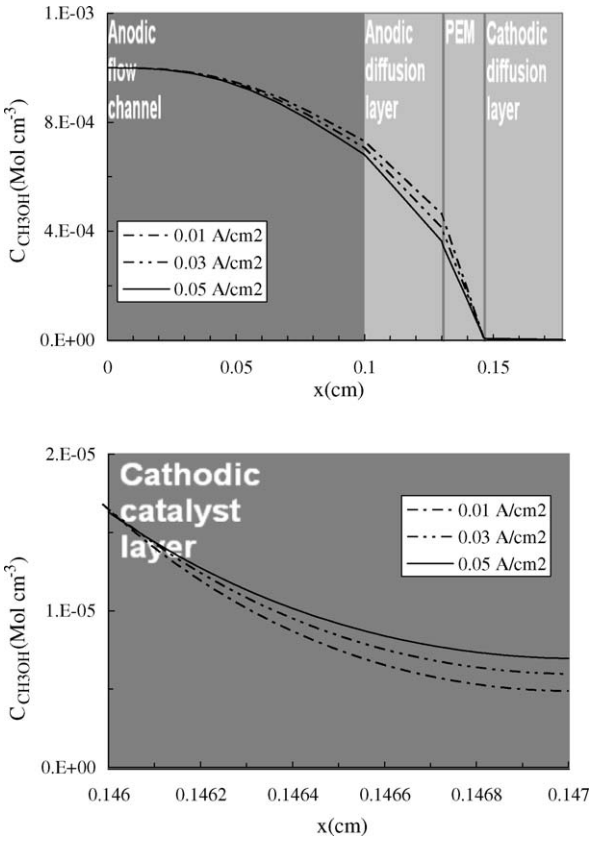

Fig. 4. Model-predicted methanol concentration distributions at different cell current densities with $C^{feed}_{CH_3OH} = 1$ M.

the model predicts little change in oxygen concentration. Therefore, we do not present oxygen concentration distributions here. Because electrochemical reactions only occur in the catalyst layers, methanol flux is constant in the diffusion layers and the PEM, as shown in Fig. 5. We also note that higher cell current densities give lower methanol permeation rates and thus better fuel efficiencies.

For this particular cell, the catalyst efficiency on methanol oxidation is considered poor but still good enough to deplete most of the methanol that permeates to the cathode, as shown in Fig. 5. However, the fraction of methanol that escapes into the air would increases if the catalyst efficiency is reduced. To manifest this phenomenon with our model, we deliberately change the catalyst efficiency of the cathode by defining the following cases:

CASE_1 $j^{c,ref}_{0,CH_3OH}$ and $j^{c,ref}_{0,O_2}$ are as listed in Table 2.
CASE_0.25 $j^{c,ref}_{0,CH_3OH}$ and $j^{c,ref}_{0,O_2}$ are multiplied by 0.25.
CASE_4 $j^{c,ref}_{0,CH_3OH}$ and $j^{c,ref}_{0,O_2}$ are multiplied by 4.

The methanol concentration distributions and the methanol flux of these cases are shown in Fig. 6. In CASE_1 only a small fraction of methanol penetrates the cathodic catalyst layer, reaches the cathodic flow channel, and escapes into the air. In CASE_0.25, due to the low catalyst efficiency, a large fraction of methanol escapes. While in CASE_4, all methanol oxidizes in the cathodic catalyst layer. This result indicates that, when the

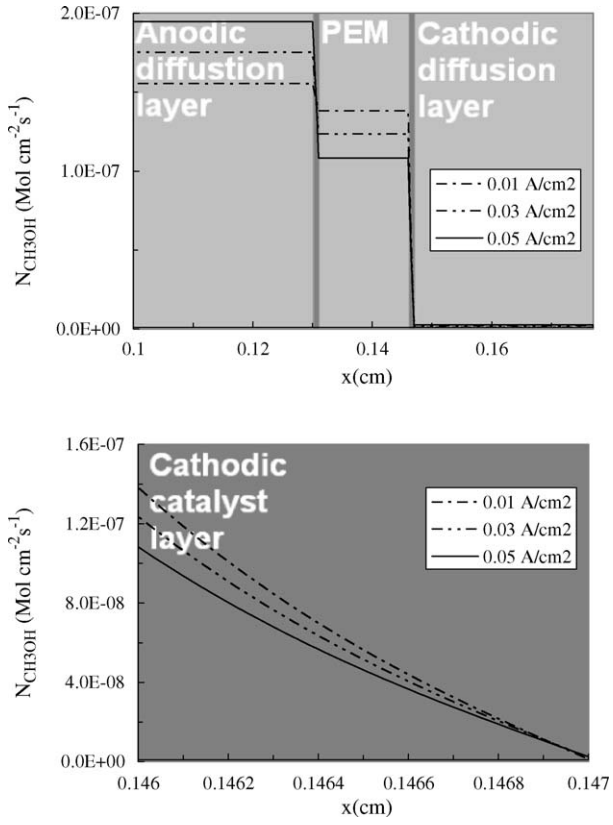

Fig. 5. Model-predicted methanol flux at different cell current densities with $C^{feed}_{CH_3OH} = 1$ M.

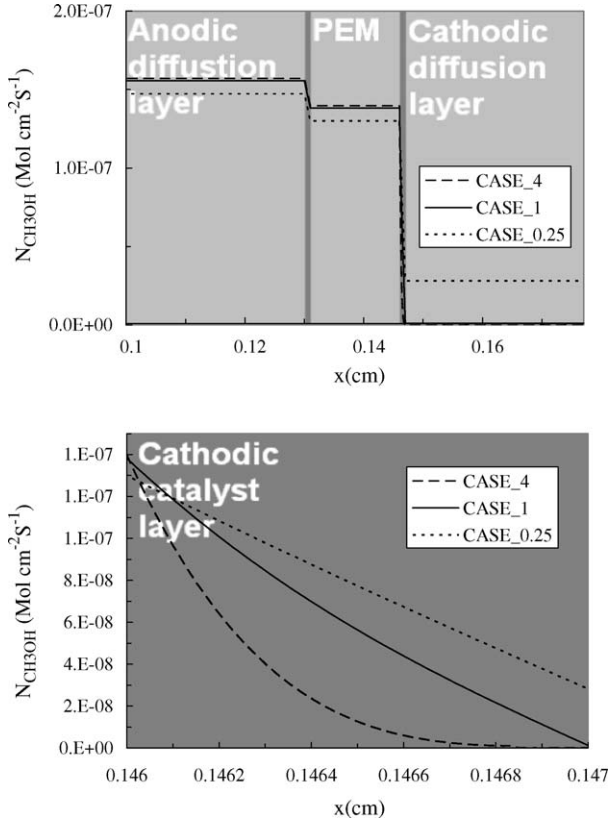

Fig. 6. Model-predicted methanol flux at different cathodic catalyst efficiencies with $C^{feed}_{CH_3OH} = 1$ M and $j_{cell} = 0.01$ A cm^2.

catalyst is not efficient, the cell output voltage that is estimated by assuming that the permeating methanol gets fully depleted in the cathode, as is done in some other models, may not be reliable.

4. Conclusions

We have developed a one-dimensional mathematical model for the DMFC which incorporates fluid dynamics calculations of the flow channels, methanol transport, oxygen transport, reaction kinetics within the anodic catalyst layer and the cathodic catalyst layer and, most important of all, the mixed potential effect. The mixed potential was calculated by means of estimating the internal current generated by methanol permeation into the cathodic catalyst layer without making the usual assumption as found in the literature that methanol transport is completely depleted in the cathodic catalyst layer. Predicting whether methanol can reach the cathodic flow channel, vaporize and exit the cell is also made possible.

We have also validated our model by an experiment with a home-assembled cell. Key parameter values of the model for this particular cell are determined through calibration which involves fitting of *I–V* characteristic curves to experimental data. With key parameter values known, we have estimated the mixed potential effect and predicted methanol concentration distributions and methanol flux inside the cell at different cell current densities.

We have also pointed out by a case study that predicting cell output voltage by assuming that methanol transfer gets depleted in the cathodic catalyst layer is not always reliable, especially when the catalyst is not efficient.

Acknowledgements

This research is sponsored by National Science Council under contract numbers 94-2218-E-007-018 and 93-2218-E-007-026 and by Institute of Nuclear Energy Research under contract number 942001INER012. We would like to thank Chao-Yuan Chiang who performed the experiment and provided the experimental data needed for this paper.

Appendix A. Fluid dynamics for the flow channels

We only consider laminar flow in a region of the flow channel where velocity and concentration are fully developed. The two-dimensional momentum equations are

$$\rho\left(u\frac{\partial u}{\partial x} + v\frac{\partial u}{\partial y}\right) = F_x - \frac{\partial P}{\partial x} + \mu\left(\frac{\partial^2 u}{\partial x^2} + \frac{\partial^2 u}{\partial y^2}\right), \quad \text{(A1)}$$

$$\rho\left(u\frac{\partial v}{\partial x} + v\frac{\partial v}{\partial y}\right) = F_y - \frac{\partial P}{\partial y} + \mu\left(\frac{\partial^2 v}{\partial x^2} + \frac{\partial^2 v}{\partial y^2}\right), \quad \text{(A2)}$$

where F_x and F_y are, respectively, the body forces acting on the fluid in the x and y directions, u and v the velocity components in the x and y directions, respectively, P the pressure, ρ the density and μ the drag coefficient.

Eq. (A1) can be neglected by applying $u = 0$. Eq. (A2) can be simplified to

$$\frac{\partial P}{\partial y} = \mu \left(\frac{\partial^2 v}{\partial x^2} \right), \tag{A3}$$

by applying $\frac{\partial v}{\partial y} = 0$ and $F_y = 0$. Assume $\frac{\partial P}{\partial y} = \text{const}$, $v(x)$ is found to be

$$v(x) = ax^2 + bx + c,$$

where a, b and c are constants. With boundary conditions $v(0) = 0$ and $v(l) = 0$, we have

$$v(x) = \frac{6f}{\mathrm{d}l^3} x(l - x), \tag{A4}$$

where l is the depth of the flow channel, d the width of the flow channel and $f \equiv d \int_0^l v \, \mathrm{d}x$ the flow rate.

The two-dimensional mass equation is

$$\left(u \frac{\partial C}{\partial x} + v \frac{\partial C}{\partial y} \right) = D \left(\frac{\partial^2 C}{\partial x^2} + \frac{\partial^2 C}{\partial y^2} \right), \tag{A5}$$

where u and v are the velocity components in the x and y directions, respectively, C the concentration and D the diffusion coefficient.

After applying $u = 0$ and neglecting $\frac{\partial^2 C}{\partial y^2}$ by assuming that variation of C along y is minimal, the mass equation is simplified to

$$v \frac{\partial C}{\partial y} = D \frac{\partial^2 C}{\partial x^2}. \tag{A6}$$

The dependences of C on x and y can be isolated by assuming $C(x,y) = C_x(x)C_y(y)$ and introducing a constant w which is to be determined by boundary conditions. $C_y(y)$ is found to be

$$C_y(y) = \exp(-y/w), \tag{A7}$$

and Eq. (A6) becomes

$$\frac{\partial^2 C_x}{\partial x^2} = -\frac{v}{wD} C_x = -\frac{6f}{wDdl^3} x(l - x) C_x. \tag{A8}$$

Define $N_x \equiv -D \frac{\partial C_x}{\partial x}$, Eq. (A8) becomes

$$\frac{\partial N_x}{\partial x} = \frac{6f}{wdl^3} x(l - x) C_x. \tag{A9}$$

Applying Eq. (A9) to our one-dimensional model we get Eqs. (2), (28) and (30).

References

[1] K. Scott, P. Argyropoulos, K. Sundmacher, A model for the liquid feed direct methanol fuel cell, J. Electroanal. Chem. 477 (1999) 97–110.

[2] K.T. Jeng, C.W. Chen, Modeling and simulation of a direct methanol fuel cell anode, J. Power Sources 112 (2002) 67–375.

[3] J.P. Meyers, J. Newman, Simulation of the direct methanol fuel cell. I, J. Electrochem. Soc. 149 (2002) A710–A717.

[4] J.P. Meyers, J. Newman, Simulation of the direct methanol fuel cell. II, J. Electrochem. Soc. 149 (2002) A718–A728.

[5] J.P. Meyers, J. Newman, Simulation of the direct methanol fuel cell. III, J. Electrochem. Soc. 149 (2002) A729–A735.

[6] J. Divisek, J. Fuhrmann, K. Gärtner, R. Jung, Performance modeling of a direct methanol fuel cell, J. Electrochem. Soc. 150 (2003) A811–A825.

[7] J.J. Baschuk, X. Li, J. Power Sources 86 (2000) 181.

[8] C. Marr, X. Li, ARI 50 (1998) 190.

[9] C.W. Tobias, Advances in Electrochemistry and Electrochemical Engineering, Wiley, New York, 1962, p. 19.

[10] E.L. Cussler, Diffusion: Mass Transfer in Fluid Systems, Cambridge University Press, New York, 1984.

[11] C.L. Yaws, Handbook of Transport Property Data: Viscosity, Thermal Conductivity and Diffusion Coefficients of Liquids and Gases, Gulf Pub Co, Houston, TX, 1995.

[12] X. Ren, W. Handerson, S. Gottesfeld, J. Electrochem. Soc. 144 (9) (1997) L267.

[13] K. Scott, W. Taama, J. Cruickshank, J. Power Sources 65 (1997) 159.

[14] A. Parthasarathy, S. Srinivasan, A.J. Appleby, J. Electrochem. Soc. 139 (1992) 2530.

[15] S.F. Baxter, V.S. Battaglia, R.E. White, J. Electrochem. Soc. 146 (2) (1999) 437.

[16] T.A. Zawodzinski, M. Neeman, L.D. Sillerud, S. Gottesfeld, J. Phys. Chem. 95 (1991) 6040.

[17] Z.H. Wang, C.Y. Wang, Mathematical modeling of liquid-feed direct methanol fuel cells, J. Electrochem. Soc. 150 (2003) A508–A519.